Loss Distribution and Thermal Behaviour of the Y-source Converter for a Wide Power and Voltage Range

Gadalla, Brwene Salah Abdelkarim; Schaltz, Erik; Siwakoti, Yam Prasad; Blaabjerg, Frede

Published in:
Proceedings of 2017 IEEE 3rd International Future Energy Electronics Conference and ECCE Asia (IFEEC 2017 - ECCE Asia)

DOI (link to publication from Publisher):
10.1109/IFEEC.2017.7992156

Publication date:
2017

Document Version
Early version, also known as pre-print

Loss Distribution and Thermal Behaviour of the Y-source Converter for a Wide Power and Voltage Range

Brwene Gadalla[1,2], Erik Schaltz[1], *Member IEEE*, Yam Siwakoti [3], *Member IEEE*, Frede Blaabjerg[1], *Fellow IEEE*
[1]Department of Energy Technology, Aalborg University
Aalborg 9220, Denmark
[2]Electrical and Computer control Department, Arab Academy for Science, technology and maritime transport
Cairo, Egypt
[3]Department of Electrical, Mechanical and Mechatronic Systems
University of Technology Sydney
Sydney, Australia
bag@et.aau.dk, bruin.elkarim@staff.aast.edu, esc@et.aau.dk, Yam.Siwakoti@uts.edu.au, fbl@et.aau.dk

***Abstract*—The Y-source converter is one of the recent proposed impedance source converters. It has some advantages as having a high voltage gain between the input and output voltage sides using very small duty cycle ratios. For many applications, the input voltage needs to be boosted to higher output voltage, such as for fuel cell, battery electric vehicles and renewable energy applications. Understanding the loss distribution and thermal performance is very important in order to be able to design a reliable converter with longer lifetime. In this paper, the loss distribution of a Y-source converter for a wide voltage and power range is presented. The influence of the heat losses generated in the converter is also considered for different analysis. A simulation model is developed and verified experimentally rated at 300 W.**

I. Introduction

Power converters have been used in many renewable energy applications [1] and more recently with electric vehicles [2] and fuel cell applications [3], which require high voltage gain. Researchers have claimed that impedance source converter has its uniquely advantages such as, having a high voltage gain in the small range of duty cycle and more degree of freedom for setting the voltage gain as needed for a specific application. A collective investigation has been achieved for the Y-source converter [4], [5] and compared with other [6] (conventional boost and Z-source) converters with respect to the thermal and efficiency performances. However, to our knowledge the loss distribution has not been validated experimentally yet.

The Y-source converter circuit diagram and it's two modes of operations are shown in Fig. 1. It is realized by a three-winding coupled inductor (N_1, N_2, and N_3), an active switch SW, two diodes (D_1, D_2), a capacitor C_1 [6], [7]. Due to the discontinuity nature of the current in winding N_1, an input

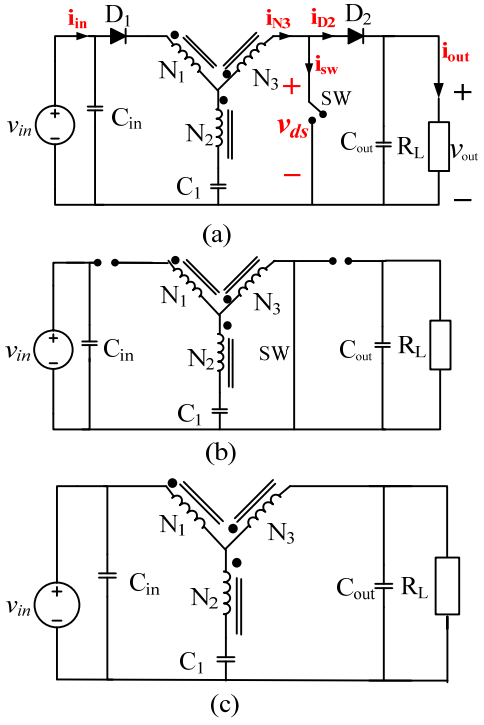

Fig. 1. Boost circuit topology a) Y-source converter equivalent circuit. b) Equivalent circuit for on state. c) Equivalent circuit for off state.

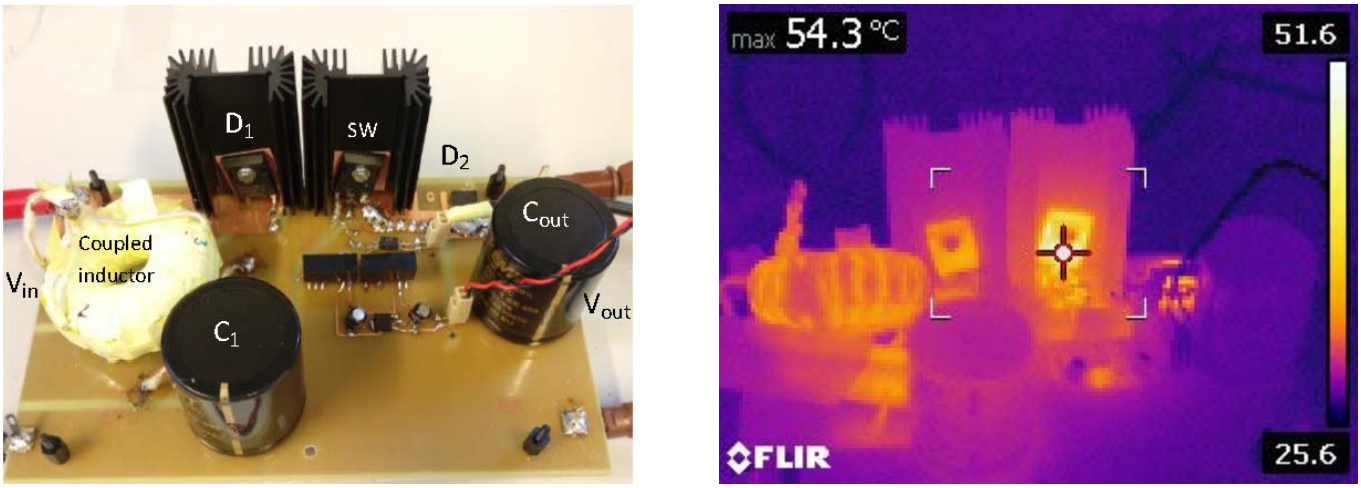

(a) (b)

Fig. 2. a) Experimental set-up of Y-source converter. b) Thermal image of the prototype Y-source converter operating at nominal load.

capacitor was added in the prototype to smoothen the input current. However, other variations of the Y-source converter which provide a constant input current also exist [8].

II. METHODOLGY

In order to analyse the loss distribution and the efficiency of the converter a prototype of the Y-source converter has been built at 300 W rated power which is shown in Fig. 2(a). The thermal image of the converter shown in Fig. 2(b) reflect the case temperature of all the components in the converter during operation. FLIR thermal camera is used, where it is seen that the highest temperature is of the switch (MOSFET) which indicates a high loss.

In Table I all parameters used in both the simulation model and the prototype design are shown. For the inductor characertics, an MPP core [9] type used, which has the advantage of having lower losses than other types as ferrite cores. Different power loadings are considered for the loss distribution investigation. These losses can be listed as switching, conduction, capacitor ESR, core and winding losses [6] [10].

In Table II the design formulas of the passive elements (inductor and capacitor) are shown.

Furthermore, the thermal performance is also considered, since the junction temperature [11] is an important parameter as it affects the lifetime of the converter. PLECS toolbox is used in the results of the simulation model with different loading powers as shown in Fig. 3.

It is to be noted that the heat losses of the switch and the two diodes also is included in the simulation model in order to investigate the junction temperature.

All analysis are performed under the same operating conditions considering the ambient temperature 25 °C, the switching frequency 20 kHz and the voltage gain (G=4) as listed in Table I.

TABLE I.

Parameters used in the simulation and expermintal prototype of the Y-source converter.

Parameter	Value / description
Rated power (P)	300 W
Voltage gain	4
Winding factor (K) , $K=\frac{N_1+N_3}{N_3-N_2}$	4
Input voltage (V_{in})	60 V
Output voltage (V_{out})	240 V
Duty cycle (d_{st})	0.1875
Turns ratio of coupled inductor (N_1:N_2:N_3)	5:1:3
No. of turns (N_1:N_2:N_3)	80:16:48
Core	MPP C055863A2
Switching frequency (f_s)	20 kHz
Capacitors	C_{in} = 470 µF, 400 V Kemet C_1 = 470 µF, 400 V Kemet C_2 = 470 µF, 400 V Kemet
Switch (Mosfet)	C2M0040120D, 1200v, 60 A
Diode D_1	C3D25170H, 1700v, 26.3 A
Diode D_2	C3D20060D, 600v, 20 A

TABLE II.

Passive component design in the Y-source converter.

Passive Components	Y-source
Inductor	$L_N = A_L N^2 10^{-3}$, $L_{lik}=\frac{0.292\times N^{1.056}\times A_c}{L_c}$ $L = L_N + L_{lik}$
Capacitor	$C_1 \geq \frac{D}{2\%\,(1-D)\,f_s}\left(\frac{1}{1-k\,D}-1\right)\frac{P_o}{V_o^2}$ $C_{out}=\frac{V_{out}\times D}{R_l\times f_s\times \Delta V_{out}}$

L_N: Nominal inductance, L_{lik}: leakage inductance, K: winding factor

III. EVALUATION OF POWER LOSSES AND THERMAL PERFORMANCE

In this section, all the equations used in calculating the relevant power losses are presented [6], [12]. PLECS toolbox

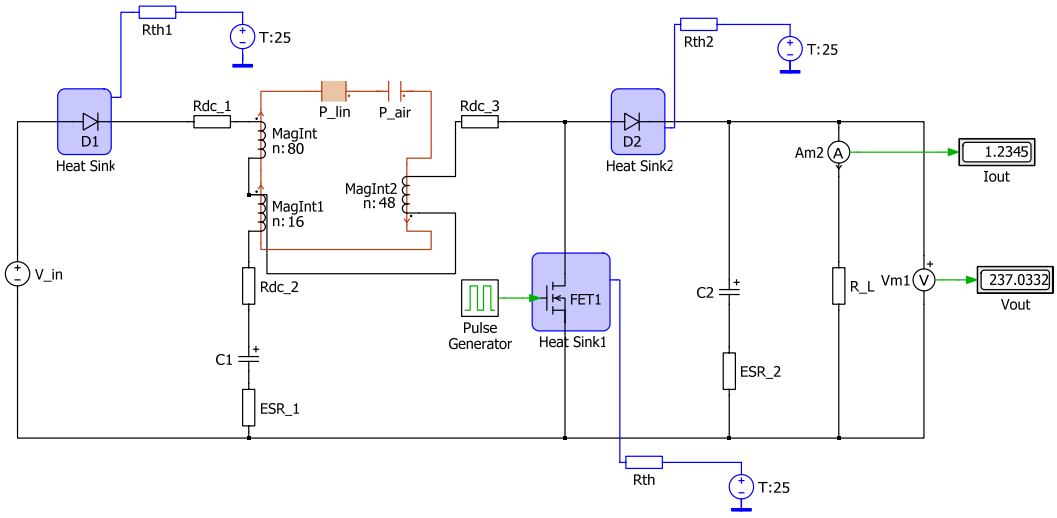

Fig. 3. PLECS model of a Y-source converter for thermal analysis.

is used for the Y-source converter analysis. Loss models are developed in PLECS and compared with the losses equations to map the losses in the simulation model.

A. Switching and conduction losses calculations

1) The MOSFET switching losses are a function of the load current and the switching frequency. The switching losses P_{sw} are expressed in (1) as:

$$P_{SW} = V_{ds} \times I_{sw} \times f_{SW} \times \frac{(Q_{GS2} + Q_{GD})}{I_G} \quad (1)$$

where V_{ds} which is the drain to source voltage, I_{sw} which is the switch (drain) current, f_{sw} is the switching frequency, Q_{GS2} is the gate source charge and Q_{GD} is the gate drain charge, and I_G is the gate current.

2) Conduction losses occur when the device is in full conduction mode. Neither of these losses are a function of the switching frequency.
The conduction losses P_{cond} are expressed in (2) as:

$$P_{cond} = R_{ds(on)} \times I^2_{sw(RMS)} \quad (2)$$

where $R_{ds(on)}$ is the resistance of the selected MOSFET, $I_{sw(RMS)}$ is the root mean square current passing through the MOSFET.

B. Capacitor ESR losses calculations

The Equivalent Series Resistance (ESR) is a parameter, which models the total effect of a large set of energy loss mechanisms in the capacitor occurring under the operating conditions through a certain value of a resistance. So the capacitors ESR losses are expressed in (3) as:

$$P_{cap.loss} = I^2_{cap.} \times ESR \quad (3)$$

where $I_{cap.}$ is the rms current passing through the capacitor, and ESR is the equivalent series resistance measuring the effect of the losses dissipated in the capacitor.

C. Winding and core losses calculations

1) The winding losses are the energy dissipated by the resistance of the wire in the coil. It can be classified into two types of losses (DC and AC winding loss). The DC winding losses can be calculated in (4) as:

$$P_{DC} = I^2_{av} \times R_{DC} \quad (4)$$

where, P_{DC} is the DC copper losses in the winding, I_{av} is the average current passing through the wire, and R_{DC} is the DC resistance of the wire.

2) AC winding losses can be significant for large current ripple and also for high frequency. It can be calculated through the skin effect, where the current density is an exponentially decaying function of the distance into the wire, with a characteristic length δ, which is known as the skin depth.

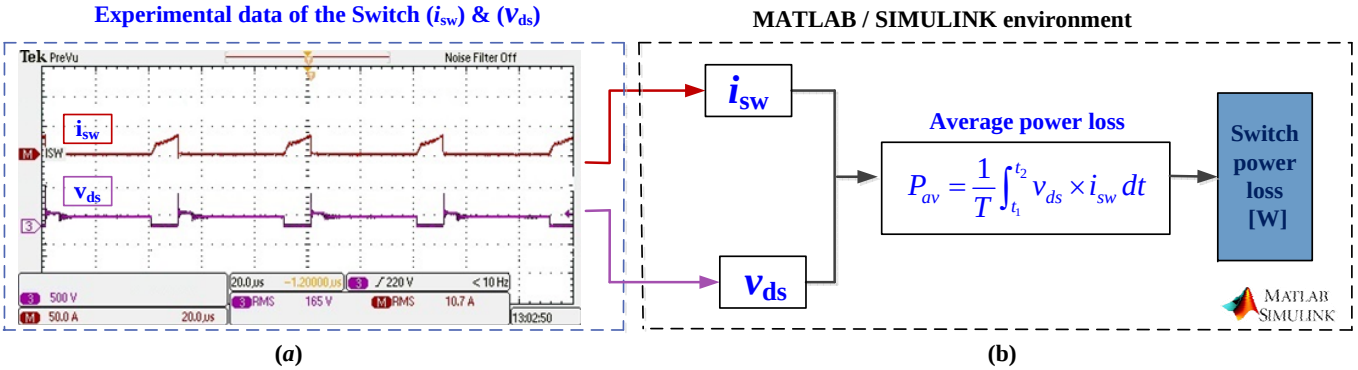

Fig. 4. Illustration diagram of switch loss calculatuion in Y-source converter prototype. a) waveform of the switch current (i_{sw}) and switch volatge (v_{ds}). b) calculation method.

In order to calculate the AC resistance R_{AC}, the thickness h of the wire should be known since it is a function of the DC resistance R_{DC} which can be calculated in (5):

$$R_{AC} = \frac{h}{\delta} \times R_{DC} \tag{5}$$

where, h is the thickness of the wire in cm and δ is the skin depth.
The AC winding losses can be calculated as given in (6):

$$P_{AC} = I_{AC-rms}^2 \times R_{AC} \tag{6}$$

Where, P_{AC} is the AC winding loss, I_{AC-rms} is AC ripple RMS current passing through the wire, and R_{AC} is the AC winding resistance.

3) According to Steinmetz's equation, which is used to calculate the core loss of magnetic materials due to magnetic hysteresis, the core losses is expressed in (7) as:

$$P_v = k f^{\alpha} \hat{B}^{\beta} \tag{7}$$

where $\hat{B}$ is the peak flux density excitation with frequency f, P_v is the time-average power loss per unit volume, and the parameters (α, β, k) are related to the material.

IV. Simulation and Expermintal Results

According to the loss distribution shown in Fig. 5 of the pie chart, and the thermal image shown in Fig. 2(b) the switch (MOSFET) is the most critical component in the Y-source converter as 76% of the total losses are generated from the switch. Therefore, it is decided to focus on validating the switch loss in the prototype.

As stated earlier, the loss calculations in the Y-source simulation model are performed through PLECS toolbox. Since the power losses of the switch could not be measured directly, the total switch loss is calculated based on the switch voltage and current measurements. Therefore, in order to validate the loss calculations in the Y- source prototype converter, the switch voltage (v_{ds}) and current (i_{sw}) waveforms obtained from the prototype are processed in Matlab as shown in Fig. 4.

A. Simulation results

In this section, starting with the initial condition as a dc input voltage source powering the converter where, V_{in}= 60 V and an input capacitor C_{in} is added in order to smoothen the input current signal and at the same time the current passing through the winding N_1, due to the discontinuity nature of the input current i_{in} of the Y-source converter.

Fig. 5 provides more detailed analysis for the amount of losses in the simulated converter at 300 W rated power and four times voltage gain. The results indicate that the switch losses is sharing 76%, the total conduction losses of the two diodes (D_1 and D_2) is 6%, the capacitor loss is 15%, and the heat loss generated from the winding loss is only 3%.

Furthermore, it is noted that reducing the power level from 300 W to 100 W has a significant influence on the loss reduction of the switch.

The results in Fig. 6 shows the losses distribution for the simulated converter at three power levels (100 W, 200 W, and 300 W) and two different voltage gains (3 and 4). The switch losses indicated in this figure are for the total losses (switching and conduction loss) generated from the MOSFET, the diodes loss is the total losses for (D_1 and D_2). In the winding loss, only the DC winding loss is presented since the AC winding loss is minimal so it is neglected. It can be seen from the losses distribution that the losses of the switch is the highest power loss at different power levels and voltage gains.

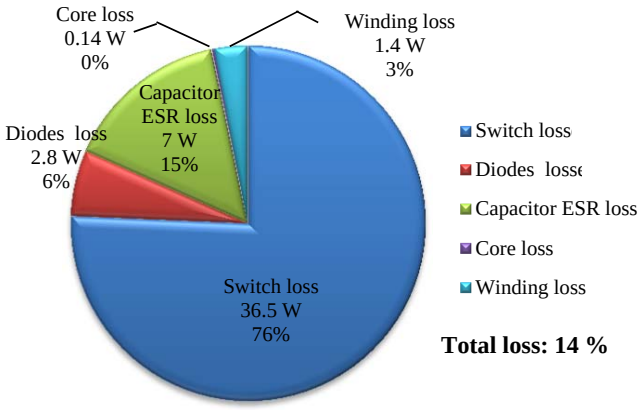

Fig. 5. Simulated power losses distribution for the Y-source converter at 300 W power loading and voltage gain of 4.

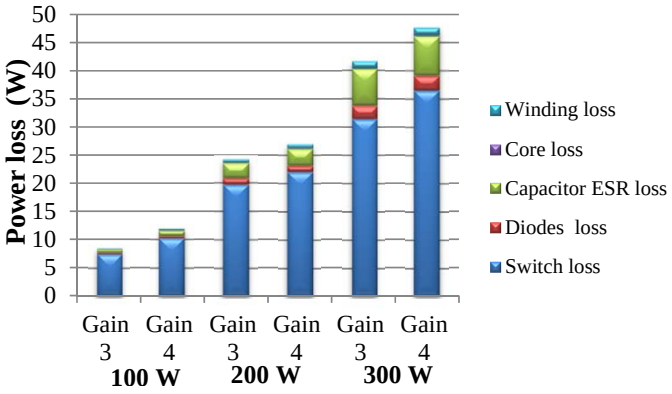

Fig. 6. Simulation results of different losses distribution for the Y-source converter at different loadings 100 W, 200 W and 300 W loading and different voltage gains (3, and 4).

B. Experimental results

The obtained waveforms are captured by a 100 MHz digital phosphor oscilloscope (DPO2014) from Textronix.

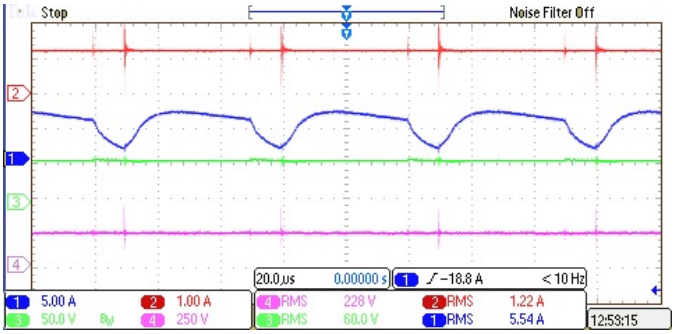

Fig. 7. Experimental waveforms of the Y-source converter with k = 4, d_{st} = 0.19 and P = 300 W at its zoom view where, Ch. 1: input current (i_{in}), Ch. 2: output current (i_{out}), Ch. 3: input voltage (v_{in}), and Ch.4: output voltage (v_{out}).

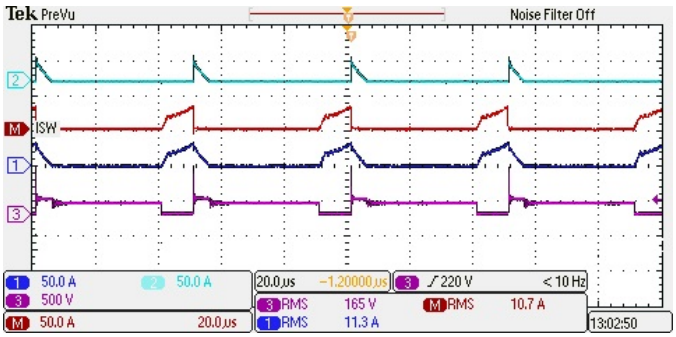

Fig. 8. Experimental waveforms of the Y-source converter with k = 4, d_{st} = 0.19 and P = 300 W at its zoom view Where, Ch. 1: current through winding N_3 , Ch. 2: current through diode D_2 (i_{D_2}), Ch. M: current through SW (i_{sw}) obtained through the math opertaion on the osciliscope, and Ch.3: drain to source voltage (v_{ds}).

In Fig. 7 different experimental currents and voltage waveforms located in the converter are presented where they are as expected under the same conditions as listed in Table I, 300 W rated power and four times gain. The input and output sides are shown ((v_{in}), (i_{in}), (v_{out}) and (i_{out})), where it matches the simulated waveforms.

In order to be able to verify the loss distribution in the Y-source converter, the measurements of the voltage and current passing through each component need to be known. Since the switch loss is the highest generated loss in the converter, two steps are taken for the validation.

First, measuring the general efficacy of the prototype output/input sides. Second, specify closer analysis for the switch losses and its thermal behaviour by including a case/junction temperature measurement.

In the first criteria, the total efficiency of the converter can be measured in both the simulation model and in the prototype from Fig. 7 where the output/input signal can be easily assign the efficiency to be $(P_{out})/(P_{in})$= 84%, while in the simulation model it is equal 86%.

Fig. 8 shows the voltage (v_{ds}) and current (i_{sw}) of the (switch) MOSFET, and the current (i_{D_2}) through diode D_2, and current (i_{N_3}) passing through the winding N_3.

The total switch current can be measured through the math operation in the oscilloscope and compared with simulated one to verify the total switch loss as shown in Fig. 6. The value of the obtained switch current (i_{sw}), which can be seen in Fig. 8 from the prototype, matches with the switch current in the simulation model and as well the same average power loss generated for the total loss of the switch. In the simulation model the total switch loss is 36.5 W, and the measured average power loss from the processed data through Matlab is 38.5 W.

Moreover, the case temperature (54.3°C) of the switch, which can be seen in the thermal image shown in Fig. 2b

matches with the expected calculated value of the simulated junction temperature (62.3°C) while using the same heat sink in both the simulation model and the prototype.

V. CONCLUSION

In this paper an investigation of the Y-source converter has been performed with respect to its thermal behaviour and loss distribution. The results show that the Y-source converter operates with high voltage gain and small duty cycle ratio. It is observed that the Y-source converter experiences high current stress in its switch, which therefore has the highest risk and must be sized appropriately. Loss distribution and case temperature measurement with respect to 300 W power level at the same ambient temperature is performed. Most of the losses in the converter was in the switch. Different power levels have been analyzed and the total power loss of the switch has been verified experimentally. The Y-source converter prototype behaves as expected compared with the simulation model.

REFERENCES

[1] J. M. Shen, H. L. Jou, and J. C. Wu, "Ripple voltage suppression method for dc/dc boost converter of the grid-connected renewable power generation system," in *Proc. of SET*, Nov. 2008, pp. 110–115.

[2] O. Hegazy, J. V. Mierlo, and P. Lataire, "Analysis, control and comparison of dc/dc boost converter topologies for fuel cell hybrid electric vehicle applications," in *Proc. of EPE*, Aug. 2011, pp. 1–10.

[3] Y. Siwakoti, P. C. Loh, F. Blaabjerg, S. Andreasen, and G. Town, "Y-source boost dc/dc converter for distributed generation," *IEEE Trans. Ind. Electron.*, vol. 62, no. 2, pp. 1059–1069, Feb. 2015.

[4] Y. Siwakoti, F. Z. Peng, F. Blaabjerg, P. C. Loh, and G. Town, "Impedance-source networks for electric power conversion part I: A topological review," *IEEE Trans. Power Electron.*, vol. 30, no. 2, pp. 699–716, Feb. 2015.

[5] Y. Siwakoti, P. C. Loh, F. Blaabjerg, and G. Town, "Y-source impedance network," in *Proc. of 29th Annual IEEE Applied Power Electronics Conference and Exposition (APEC)*, Mar. 2014, pp. 3362–3366.

[6] B. Gadalla, E. Schaltz, Y. Siwakoti, and F. Blaabjerg, "Thermal performance and efficiency investigation of conventional boost, z-source and y-source converters," in *Proc. of 16 IEEE International Conference on Environment and Electrical Engineering (EEEIC16)*, Jun. 2016, pp. 1297– 1302.

[7] B. Gadalla, E. Schaltz, F. Blaabjerg, and Y. Siwakoti, "Investigation of efficiency and thermal performance of the y-source converters for a wide voltage range," *Journal of Renewable Energy and Sustainable Development*, vol. 1, no. 2, pp. 300–305, Jan. 2016.

[8] Y. P. Siwakoti, F. Blaabjerg, and P. C. Loh, "Quasi- y-source inverter," in *Proc. of Power Engineering Conference (AUPEC), Australasian Universities*, Sep. 2015, pp. 1–5.

[9] Magnetics. Magnetics powder core catalog. [Online]. Available: http://www.mag-inc.com/company/news/new-powder-core-catalog

[10] B. Gadalla, E. Schaltz, Y. Siwakoti, and F. Blaabjerg, "Analysis of loss distribution of conventional boost, z-source and y-source converters for wide power and voltage range," *Trans. on Enviroment and Eectrical Enigneering*, vol. 2, no. 1, pp. 1–9, Jan. 2017.

[11] H. Chung, H. Wang, F. Blaabjerg, and M. Pecht, *Reliability of Power Electronics Converter Systems*. The Institution of Engineering and Technology (IET), Dec. 2015.

[12] G. Lakkast, *MOSFET power losses and how they affect power-supply efficiency*. Analog Applications Journal, Texas instrument, 2016. [Online]. Available: http://www.ti.com/lit/an/slyt664/slyt664.pdf